Available online at www.sciencedirect.com
ScienceDirect
International Journal of Thermal Sciences 46 (2007) 699–706
International Journal of Thermal Sciences
www.elsevier.com/locate/ijts

Experimental investigation of mass transfer performance with some random packings for ammonia rectification in ammonia–water absorption refrigeration systems

Jaime Sieres, José Fernández-Seara *

Área de Máquinas y Motores Térmicos, E.T.S. de Ingenieros Industriales, University of Vigo, Campus Lagoas-Marcosende Nº 9, 36310 Vigo, Spain

Received 4 February 2006; received in revised form 10 July 2006; accepted 16 September 2006

Available online 16 October 2006

Abstract

In ammonia water absorption refrigeration systems (AARS) a high efficiency purification process to remove the water content from the generated vapour is of great importance. One type of equipment to carry out this process is a packed column. Any type of detailed analysis of a packed column requires the calculation of mass transfer coefficients. Therefore, the correlations to obtain these coefficients become an essential tool for an accurate analysis and design of these devices. An experimental facility has been designed and built to analyze the ammonia–water rectification process in packed columns. In this paper a brief description of the experimental facility is given and the variables required to analyze the column performance are explained. An analytical method to determine mass transfer coefficients from the experimental data is developed. Results of mass transfer coefficients for 15 mm glass Raschig rings, $\frac{1}{2}''$ ceramic Berl saddles and $\frac{1}{2}''$ ceramic Novalox saddles random packings are reported. The experimental results are compared with different mass transfer correlations proposed in the literature. In the paper corrected correlations are proposed for the packings considered. These correlations could be used to analyze and design a packed column for AARS.

Keywords: Mass transfer coefficients; Packed column; Random packing; Rectification; Ammonia–water; Absorption refrigeration

1. Introduction

Ammonia–water absorption refrigeration systems (AARS) constitute an old technology that has been in use since the middles of the nineteenth century [1]. From the beginning, its development has been linked to the evolution of the energy prices and mainly to the expansion of the compression refrigeration systems. As the energy prices increased and the compression systems expanded, the applications for AARS decreased. Therefore, its applications had been reduced to high cooling power plants powered by cheap or waste heat. However, for the last three decades the scenario has changed mainly due to the relation of the chlorofluorocarbon refrigerants used in compression systems with the depletion of the ozone layer [2,3]. The solution of this problem is still not clear, but one of its obvious consequences has been a renewed interest on absorption systems [4]. On the other hand, the widespread use of cogeneration plants has also contributed to the renascence of this technology, mainly in the branch of high cooling power machines [5,6].

Nowadays, the AARS are widely used in refrigeration applications (from 0 to −60 °C) with cooling powers higher than 100 kW [7]. There is also a commercial branch of small power machines for air conditioning and heat pump applications powered by direct gas fired [8]. However, it is noteworthy the lack of small machines for refrigeration (cooling production below 0 °C) that could be powered by waste heat or solar energy. The development of this type of AARS requires improving the present day technology in order to obtain more efficient and reliable components and to reduce the size and the cost of these systems as much as possible. These efforts are worthwhile since they could extend the use of AARS into new applications and improve the existing machines [9–11].

AARS are strongly influenced by the property of the ammonia–water mixture of a non-negligible vapour pressure

* Corresponding author. Tel.: + 34 986 812605; fax: + 34 986 811995.
E-mail address: jseara@uvigo.es (J. Fernández-Seara).

1290-0729/$ – see front matter
doi:10.1016/j.ijthermalsci.2006.09.003

Nomenclature

a_{ef}	effective transfer area	$m^2\,m^{-3}$
a_p	packing surface area	$m^2\,m^{-3}$
a_w	wetted surface area	$m^2\,m^{-3}$
d_c	column diameter	m
d_p	nominal size of packing	m
D	diffusion coefficient	$m^2\,s^{-1}$
g	gravitational constant	$m\,s^{-2}$
k_m	mass transfer coefficient	$m\,s^{-1}$
F	mass transfer coefficient	$kmol\,m^{-2}\,s^{-1}$
H	height of the packed section	m
$\dot{L}$	liquid superficial molar flow	$kmol\,m^{-2}\,s^{-1}$
$\dot{M}$	mass flow	$kg\,s^{-1}$
$\dot{n}$	molar flux	$kmol\,m^{-2}\,s^{-1}$
p	pressure	bar
Re	Reynolds number	
Sc	Schmidt number	
Sh	Sherwood number	
T	temperature	K
u	superficial velocity	$m\,s^{-1}$
$\dot{V}$	vapour superficial molar flow	$kmol\,m^{-2}\,s^{-1}$
x	ammonia mass concentration	$kg\,kg^{-1}$
$\bar{x}$	ammonia molar concentration	$kmol\,kmol^{-1}$
y	vertical coordinate	m
z	ratio of ammonia molar flux to total molar flux transferred	
$\bar{z}$	average value of z along the column	

Greek symbols

ε_p	void fraction of packing	
μ	dynamic viscosity	$kg\,m^{-1}\,s^{-1}$
ρ	density	$kg\,m^{-3}$
$\bar{\rho}$	molar density	$kmol\,m^{-3}$
σ	surface tension	$N\,m^{-1}$
σ_c	critical surface tension of packing material	$N\,m^{-1}$

Subscripts

i	interface
l	liquid
lm	logarithmic mean
o	overall
v	vapour

Superscripts

$*$	vapour in equilibrium with liquid

of water compare to the vapour pressure of ammonia in the generation process. The water carried over from the generator reaches the evaporator where it tends to accumulate. The presence of water in the evaporator strongly deteriorates the system performance and efficiency, as pointed out by Bogart [12] and analyzed and quantified by Fernández-Seara and Sieres [13]. Therefore, the achievement of a high efficiency purification process to remove the water content from the generated vapour is of great importance in AARS. Moreover, its significance increases as the evaporation temperature decreases [13].

In high power AARS, the purification process is carried out by a distillation column with total or partial condensation. If partial condensation is used, then a rectifier will be placed at the column top. The distillation columns used in AARS are usually of the plate's type and the rectifier consists of a shell and tubes heat exchanger [14]. In small size direct fired commercial machines, the purification process is carried out using a small plate distillation column over the generator and a helical coil rectifier [8].

Distillation columns are standard devices in chemical engineering systems for very different types of processes. In a distillation column, a counter-current contact is established between an upward vapour flow and a downward liquid flow. The intimate contact between the vapour and liquid is established by means of plates or by using different types of packings. Packed columns are not commonly used in AARS up to date. However, packed columns are easy to manufacture and usually cheaper than plates' columns. Packings can consist either of dumped or of stacked elements, or of regular packing units of the same diameter as the column [15]. Packings are available on the market in a great variety of shapes, materials and sizes. Irregular packings of small size are an interesting option to use in distillation columns for AARS since they can provide cheap and easy to fabricate columns.

The analysis of an AARS considering a distillation column with different configurations operating at complete or partial condensation is reported in Fernández-Seara et al. [16]. Detailed theoretical analysis of the heat and mass transfer processes in packed columns for AARS have been carried out in Fernández-Seara et al. [17] and Sieres and Fernández-Seara [18]. However, any type of detailed study always requires the calculation of the heat and mass transfer coefficients. Therefore, the correlations to obtain mass transfer coefficients become an essential tool for an accurate design of these devices. Moreover, parametric analyses carried out in ammonia–water packed distillation columns [17] show that the mass transfer coefficient in the vapour phase F_v has a decisive influence on the column performance. Therefore, the knowledge of this coefficient is of great importance for a correct design of the packed column and experimentally based correlations at typical operating conditions of an ammonia–water absorption refrigeration system would be of great interest.

Several researchers have reported models and correlations describing the performance of columns containing random packings. Recently, Wang et al. [19] have presented a review of mass-transfer correlations for packed columns. In the case of random packings, the first and still widely used correlations for mass transfer were developed by Onda et al. [20], who assumed that the wetted surface area is equal to the effective mass transfer area. Bravo and Fair [21] provided a new correlation of effective transfer area based on the model of Onda et al. [20], using distillation data results of Bolles and Fair [22].

Billet and Schultes [23] developed mass transfer correlations based on a physical model for packed counter-current columns filled with dumped or arranged packings. Their model requires specific constants depending on the packing type, material and dimensions. Finally, Piché et al. [24] proposed a set of artificial neural network correlations for counter-current gas–liquid packed columns based on a large experimental database.

Though many mass transfer correlations are published in the open literature, detailed experimental studies of the ammonia purification process in packed columns at normal operating conditions in AARS have not been found. Moreover, when the available correlations are applied to this application quite different results are obtained. Therefore, it was considered necessary to perform experimental validation of the current mass transfer models for random packings applied to the ammonia purification process in ammonia–water absorption refrigeration systems.

An experimental facility has been designed and built to analyze the ammonia–water rectification process in packed columns. In this paper a brief description of the experimental facility is given and the variables required to analyze the column performance are explained. An analytical method is developed to determine mass transfer coefficients from the data measured in the experimental setup. Results of mass transfer coefficients for 15 mm glass Raschig rings, $\frac{1}{2}''$ ceramic Berl saddles and $\frac{1}{2}''$ ceramic Novalox saddles random packings are reported. The experimental results are compared with different mass transfer correlations proposed in the literature.

2. Experimental setup

An experimental facility to study the ammonia–water rectification process in packed columns has been designed and built in our laboratory. The facility operates at the normal operating conditions found in the high pressure stage of small power AARS. A rectifying packed column of 0.08 m inner diameter and 0.48 m packed length has been tested at total reflux conditions. Specific components and dimensions of the experimental facility are described in detail in Sieres et al. [25] and Sieres [26].

The experimental setup has been equipped with the appropriate instrumentation, however only some variables are required to study the packed column performance which are indicated next. The liquid reflux conditions entering the column are measured with a Coriolis flow meter (M1) with typical accuracy of ±0.1% in mass flow, ±0.5 kg m^{-3} in density and ±1 °C in temperature. The liquid mass flow, density and temperature of the bottom product (liquid leaving the column) are also measured with a Coriolis flow meter (M2) with typical accuracy of ±0.2% in mass flow, ±2.0 kg m^{-3} in density and ±1 °C in temperature. The system pressure is measured with a pressure transducer of accuracy ±0.5% at full scale. The vapour outlet temperature is measured with a PT100 type A sensor.

The vapour outlet ammonia concentration is calculated from the system pressure, the vapour outlet temperature ($T_{v,out}$) and assuming saturation conditions, according to Eq. (1). The bottom liquid concentration is obtained from the density and temperature measured by the Coriolis flow meter (M2), according to Eq. (2). State equations used for the ammonia–water equilibrium and thermodynamic properties have been obtained from Ziegler and Trepp [27].

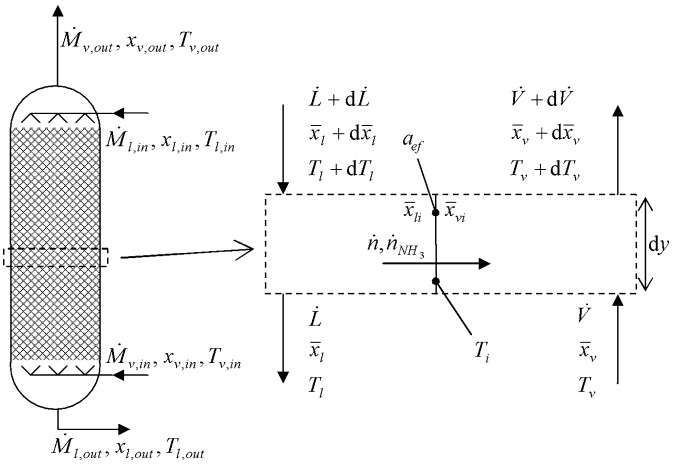

Fig. 1. Schematic diagram of the packed column and control volume for a differential packed section.

$$x_{\mathrm{v,out}} = f_{\mathrm{v,sat}}(p, T_{\mathrm{v,out}}) \tag{1}$$

$$x_{\mathrm{l,out}} = f_{\mathrm{l,sat}}(T_{M2}, \rho_{M2}) \tag{2}$$

As mentioned, the column operates at total reflux, thus the liquid reflux and vapour outlet mass flows and ammonia concentrations must be the same, according to Eqs. (3) and (4) and Fig. 1. Similarly, the vapour inlet mass flow and ammonia concentration are equal to the bottom liquid flow values, as stated in Eqs. (5) and (6).

$$\dot{M}_{\mathrm{v,out}} = \dot{M}_{\mathrm{l,in}} = \dot{M}_{\mathrm{M1}} \tag{3}$$

$$x_{\mathrm{l,in}} = x_{\mathrm{v,out}} \tag{4}$$

$$\dot{M}_{\mathrm{v,in}} = \dot{M}_{\mathrm{l,out}} = \dot{M}_{\mathrm{M2}} \tag{5}$$

$$x_{\mathrm{v,in}} = x_{\mathrm{l,out}} \tag{6}$$

Thus, from these equations, the inlet and outlet conditions of the vapour and liquid currents can be determined from the measured data.

3. Determination of mass transfer coefficients

Mass transfer between the vapour and the liquid phases results from the combined contribution of molecular diffusion and a bulk transport of material through the interface [28]. According to the film model, the molar flux of ammonia transferred from the liquid to the vapour phase can be obtained from Eq. (7) [17,28], where z is defined as the ratio of the ammonia molar flux to the net molar flux, according to Eq. (8).

$$\dot{n}_{\mathrm{NH_3}} = F_{\mathrm{v}} \cdot z \cdot \mathrm{Ln}\left(\frac{z - \bar{x}_{\mathrm{v}}}{z - \bar{x}_{\mathrm{vi}}}\right) \tag{7}$$

$$z = \frac{\dot{n}_{\mathrm{NH_3}}}{\dot{n}} = \frac{\dot{V} \cdot \mathrm{d}\bar{x}_{\mathrm{v}} + \mathrm{d}\dot{V} \cdot \bar{x}_{\mathrm{v}}}{\mathrm{d}\dot{V}} \tag{8}$$

For the characteristics operating conditions found in a rectifying packed column of an ammonia–water absorption refrigeration system, it can be shown [17] that the heat transfer resistance in the vapour phase is much higher than in the liquid phase and also that the slope of the equilibrium curve of vapour and liquid compositions is very low on a diagram with horizontal axis $\bar{x}_l$ and vertical axis $\bar{x}_v$. Therefore, it can be assumed that the interface temperature equals the liquid bulk temperature [17] and that the vapour interface concentration is approximately equal to the concentration of a vapour $\bar{x}_v^*$ that would be in equilibrium with the bulk liquid $\bar{x}_l$. Under these conditions, the overall vapour mass transfer coefficient can be considered equal to the single phase coefficient $F_{ov} \approx F_v$ [26,29].

Global mass and ammonia balances in the vapour phase applied to a differential cross-section of the packed column [17], as shown in Fig. 1, yields Eqs. (9) and (10).

$$d\dot{V} = \dot{n} \cdot a_{ef} \cdot dy \tag{9}$$

$$d(\dot{V} \cdot \bar{x}_v) = \dot{n}_{NH_3} \cdot a_{ef} \cdot dy \tag{10}$$

Combining Eqs. (7) to (10) yields Eq. (11) which gives the differential column height dy required for a differential ammonia concentration enrichment in the vapour phase $d\bar{x}_v$. In this equation $\Delta\bar{x}_{v,lm}$ is the logarithmic mean driving force given by Eq. (12).

$$dy = \frac{\dot{V}}{F_v \cdot a_{ef}} \cdot \frac{\Delta\bar{x}_{v,lm}}{(z - \bar{x}_v)} \cdot \frac{d\bar{x}_v}{(\bar{x}_v^* - \bar{x}_v)} \tag{11}$$

$$\Delta\bar{x}_{v,lm} = \frac{\bar{x}_v^* - \bar{x}_v}{\ln(\frac{z-\bar{x}_v}{z-\bar{x}_v^*})} \tag{12}$$

Analytical integration of Eq. (11) is possible assuming some simplifications. First, the Wiegand [30] approximation in which the logarithmic mean concentration difference is approximated to the arithmetic mean is considered, as expressed by Eq. (13). Second, an average value of z, obtained from global mass and species balances over the packed column as stated in Eq. (14), is used instead of the local value of z. Thus, the local value of the vapour superficial molar flow $\dot{V}$ can be obtained from Eq. (15). Finally, in the range 7 bar $< p <$ 16 bar and $0.87 < \bar{x}_l < 1$, the equilibrium vapour concentration $\bar{x}_v^*$ can be obtained accurately from Eq. (16), where the constants b_0, b_1 and b_2 are given in Table 1.

$$\Delta\bar{x}_{v,lm} \approx (z - \bar{x}_v) + \frac{\bar{x}_v - \bar{x}_v^*}{2} \tag{13}$$

$$\bar{z} = \frac{\dot{V}_{out} \cdot \bar{x}_{v,out} - \dot{V}_{in} \cdot \bar{x}_{v,in}}{\dot{V}_{out} - \dot{V}_{in}} \tag{14}$$

$$\dot{V} = \dot{V}_{out} \cdot \frac{\bar{z} - \bar{x}_{v,out}}{\bar{z} - \bar{x}_v} \tag{15}$$

Table 1
Constants

$b_0 = -9.48596 \cdot 10^{-5}$	$B = b_0 + b_1 \cdot p + b_2 \cdot p^2$
$b_1 = 6.79315 \cdot 10^{-5}$	$N_1 = \frac{1}{(1-B)\cdot(\bar{z}-1)}$
$b_2 = 9.58238 \cdot 10^{-6}$	$N_2 = \frac{1}{(1-B)\cdot(1-\bar{z})}$

$$\bar{x}_v^* = 1 - \left(b_0 + b_1 \cdot p + b_2 \cdot p^2\right) \cdot (1 - \bar{x}_l) = 1 - B \cdot (1 - \bar{x}_l) \tag{16}$$

The column operates at total reflux, then the equalities expressed in Eqs. (17) and (18) are satisfied throughout the column.

$$\dot{V} = \dot{L} \tag{17}$$

$$\bar{x}_v = \bar{x}_l \tag{18}$$

Substitution of all these expressions into Eq. (11) yields Eq. (19), where $f(\bar{x}_v)$ is given by Eq. (20).

$$dy = \frac{\dot{V}_{out} \cdot (\bar{z} - \bar{x}_{v,out})}{F_v \cdot a_{ef}} \cdot f(\bar{x}_v) \cdot d\bar{x}_v \tag{19}$$

$$f(\bar{x}_v) = \frac{1}{1-B} \cdot \frac{1}{(\bar{x}_v - \bar{z}) \cdot (\bar{x}_v - 1)} - \frac{1}{2 \cdot (\bar{x}_v - \bar{z})^2} \tag{20}$$

After partial fractionation and subsequent integration Eq. (21) is obtained, where the constants N_1 and N_2 are given in Table 1.

$$H = \frac{\dot{V}_{out} \cdot (\bar{z} - \bar{x}_{v,out})}{F_v \cdot a_{ef}} \cdot \left[N_1 \cdot \ln\left(\frac{\bar{x}_{v,out} - \bar{z}}{\bar{x}_{v,in} - \bar{z}}\right) + N_2 \cdot \ln\left(\frac{\bar{x}_{v,out} - 1}{\bar{x}_{v,in} - 1}\right) + \frac{1}{2} \cdot \left(\frac{1}{\bar{x}_{v,out} - \bar{z}} - \frac{1}{\bar{x}_{v,in} - \bar{z}}\right)\right] \tag{21}$$

This equation gives the packing height required for a given separation. Moreover, if a packed section is experimentally tested and the inlet and outlet vapour and liquid conditions are measured, then Eq. (21) can be used to determine an average value of the volumetric mass transfer coefficient $F_v \cdot a_{ef}$; or either the mass transfer coefficient F_v or effective transfer area a_{ef} if the other parameter is known.

In this work, Eq. (21) has been used to determine experimental values of the volumetric mass transfer coefficients $F_v \cdot a_{ef}$ of a packed column for typical operating conditions found in an ammonia–water absorption refrigeration system. The inlet and outlet conditions needed in this equation are obtained experimentally as described in Section 2 of this paper.

Before applying Eq. (21) to obtain experimental results, it is interesting to evaluate the magnitude of the uncertainty of the volumetric mass transfer coefficient ($F_v \cdot a_{ef}$) as a function of the variables and instrumentation used for its determination. Table 2 shows typical uncertainties of the measured data and calculated volumetric mass transfer coefficients for three different test runs with different types of packings. The uncertainties have been determined from the accuracy specifications of the different sensors based on a propagation of uncertainty analysis as indicated in Ref. [31]. According to the results shown in Table 2, typical uncertainties of $F_v \cdot a_{ef}$ are around 5%.

Finally, in order to evaluate the effect of uncertainty in the experimental measurements on the values of $F_v \cdot a_{ef}$, the coefficients of sensibilities for case 1 of Table 2 are shown in Fig. 2. It is evident from the results presented in Fig. 2 that the uncertainties in $F_v \cdot a_{ef}$ are very sensitive to the determination of the vapour outlet concentration from the pressure and outlet temperature data. The measurement of the mass flow rate of

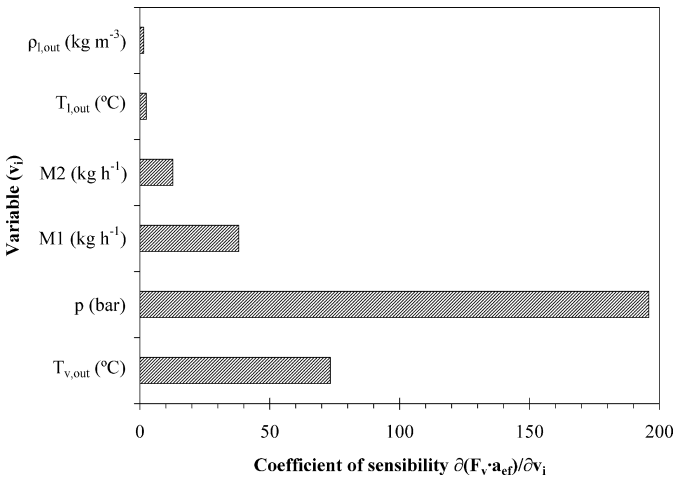

Fig. 2. Coefficients of sensibilities of the measured data on the experimental values of the volumetric mass transfer coefficient.

Table 2
Measurement uncertainties

	Case 1	Case 2	Case 3
Packing	15 mm glass Raschig ring	$\frac{1}{2}''$ ceramic Berl saddle	$\frac{1}{2}''$ ceramic Novalox saddle
$T_{v,out}$ (°C)	32.4 (0.3)	19.1 (0.3)	42.4 (0.3)
p (bar)	11.1 (0.1)	6.9 (0.1)	15.1 (0.1)
M1 (kg h^{-1})	12.60 (0.02)	12.59 (0.02)	14.41 (0.02)
$T_{l,out}$ (°C)	32.4 (0.7)	21.3 (0.6)	42.3 (0.7)
$\rho_{l,out}$ (kg m^{-3})	652.5 (1.2)	662.0 (1.2)	621.3 (1.2)
M2 (kg h^{-1})	9.1 (0.1)	8.5 (0.1)	10.1 (0.1)
$F_v \cdot a_{ef}$ (mol m^{-3} s^{-1})	600 (30)	600 (30)	610 (30)

the liquid reflux (M1) has also some effect on the uncertainty of $F_v \cdot a_{ef}$, whereas the measurements of mass flow, density and temperature of the bottom liquid (M2) have a much lower effect. Similar results were found for other test runs and with different packings.

4. Results and discussion

The random packings that have been tested are 15 mm glass Raschig rings, $\frac{1}{2}''$ ceramic Berl saddles and $\frac{1}{2}''$ ceramic Novalox saddles. The characteristic packing features are given in Table 3. Many experimental test runs have been made with the three packings considered. All the experiments were run at total reflux conditions.

The experimental values of the volumetric mass transfer coefficients $F_v \cdot a_{ef}$ have been compared with those obtained from different correlations at disposal in the literature. Fig. 3 compares the volumetric mass transfer coefficient $F_v \cdot a_{ef}$ of the 15 mm glass Raschig rings determined from the experimental results with those obtained from the correlations of Onda et al. [20], Bravo and Fair [21] and Piché et al. [24]. It can be seen that the Bravo and Fair and the Piché et al. correlations predict lower values of the volumetric mass transfer coefficients than the experimental ones. However, the Onda et al. correlation predicts the experimental mass transfer coefficients quite well. The average deviation with the experimental values is 5%.

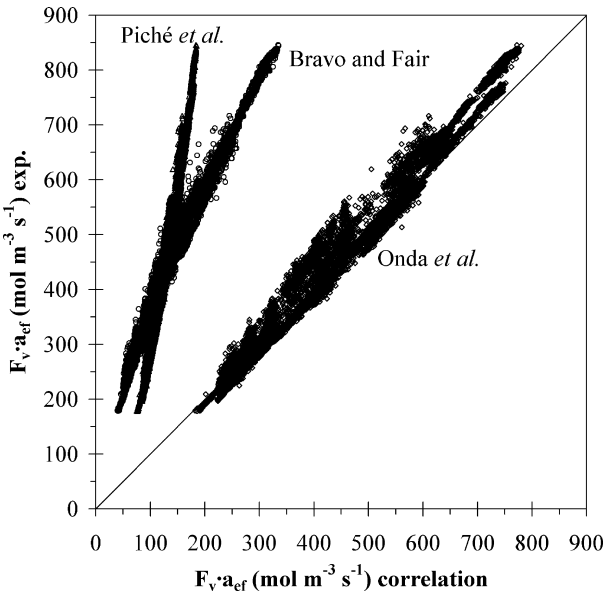

Fig. 3. Comparison between the experimental volumetric mass transfer coefficients ($F_v \cdot a_{ef}$) and predicted by the correlations of Onda et al., Bravo and Fair, and Piché et al., for 15 mm glass Raschig rings.

The analysis has been repeated with $\frac{1}{2}''$ ceramic Berl saddles and with $\frac{1}{2}''$ ceramic Novalox saddles. In Figs. 4 and 5 the experimental values of $F_v \cdot a_{ef}$ have been compared with those obtained with the Onda et al., Bravo and Fair and Piché et al. correlations. The Billet and Schultes [23] correlation was also checked for the $\frac{1}{2}''$ ceramic Berl saddles because specific constants needed in the correlation are available for this packing but not for the other two ones. Once again, the Onda et al. correlation is the one that better predicts the experimental data; however, deviations found for these two packings are greater than with 15 mm glass Raschig rings. The average deviation of the $F_v \cdot a_{ef}$ values predicted with the Onda et al. correlation and the experimental values is of 12% for $\frac{1}{2}''$ ceramic Berl saddles and 27% for $\frac{1}{2}''$ ceramic Novalox saddles. It should be noticed that the major deviations are obtained with the Novalox saddles

Table 3
Packing features

Packing type	15 mm Raschig rings	Berl saddles $\frac{1}{2}''$	Novalox saddles $\frac{1}{2}''$
Material	Glass	Ceramic	Ceramic
Nominal size (m)	0.015	0.0127	0.0127
Surface area (m^2 m^{-3})	331	465	622
Critical surface tension (N m^{-1})	0.073	0.061	0.061
Void fraction (%)	79	62	73

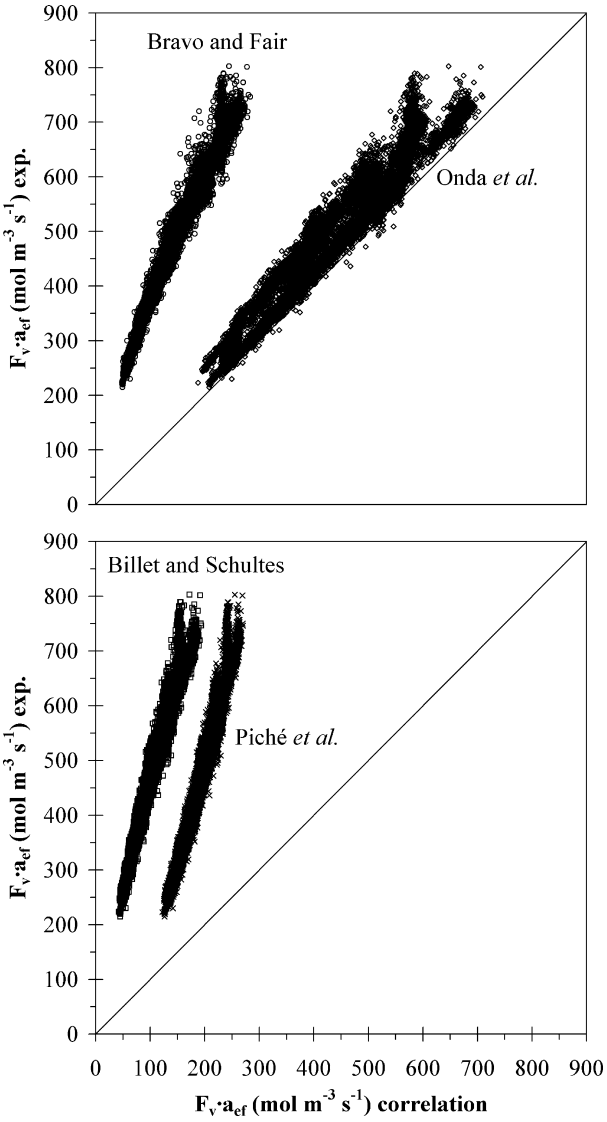

Fig. 4. Comparison between the experimental volumetric mass transfer coefficients ($F_v \cdot a_{ef}$) and predicted by the correlations of Onda et al., Bravo and Fair, Billet and Schultes, and Piché et al., for $\frac{1}{2}''$ ceramic Berl saddles.

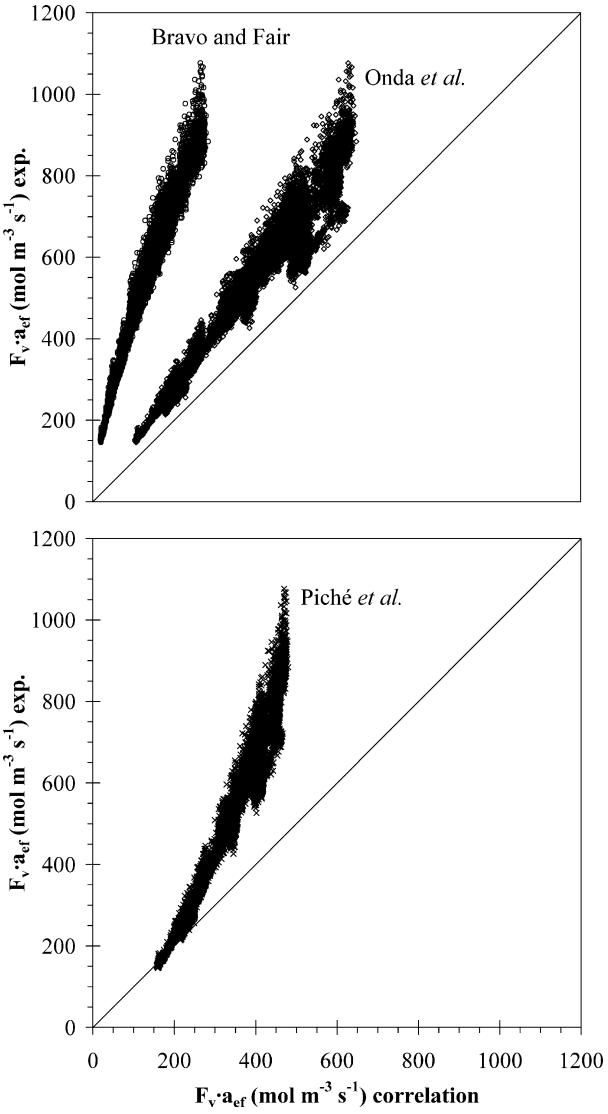

Fig. 5. Comparison between the experimental volumetric mass transfer coefficients ($F_v \cdot a_{ef}$) and predicted by the correlations of Onda et al., Bravo and Fair, and Piché et al., for $\frac{1}{2}''$ ceramic Novalox saddles.

which was not a packing type considered in the work of Onda et al.

The vapour phase mass transfer coefficient correlation proposed by Onda et al. is given in Eq. (22), whereas Eq. (23) expresses the wetted area correlation, which was used by Onda et al. as the effective transfer area.

$$Sh_v = C \cdot Re_v^{0.7} \cdot Sc_v^{0.333} \cdot (a_p \cdot d_p)^{-2} \tag{22}$$

$$\frac{a_w}{a_p} = 1 - \exp\left(-1.45 \cdot \left(\frac{\sigma_c}{\sigma_l}\right)^{0.75} \cdot \left(\frac{\rho_l \cdot u_l}{a_p \cdot \mu_l}\right)^{0.1} \cdot \left(\frac{a_p \cdot u_l^2}{g}\right)^{-0.05} \cdot \left(\frac{\rho_l^2 \cdot u_l^2}{a_p \cdot \sigma_l}\right)^{0.2}\right) \tag{23}$$

The Reynolds, Schmidt and Sherwood numbers used in Eq. (22) are defined in Eqs. (24), (25) and (26), respectively. Table 4 resumes the range of the Reynolds, Schmidt and Sherwood numbers during all the experiments carried out with the three different packings analyzed.

$$Re_v = \frac{\rho_v \cdot u_v}{a_p \cdot \mu_v} \tag{24}$$

$$Sc_v = \frac{\mu_v}{\rho_v \cdot D_v} \tag{25}$$

$$Sh_v = \frac{k_{mv}}{a_p \cdot D_v} = \frac{F_v}{a_p \cdot D_v \cdot \bar{\rho}_v} \tag{26}$$

According to Onda et al., Raschig rings and Berl saddles data are best correlated when the parameter C in Eq. (22) takes the numerical value 2.0 if the nominal packing size is less than 15 mm and the value 5.23 if the nominal packing size is equal or greater than 15 mm. Other authors [29] recommend changing the constant value C for nominal packing sizes lower than 12 mm instead of 15 mm. In this work the experimental values of the volumetric mass transfer coefficient were better predicted using the value 5.23 for the three packings analyzed.

Table 4
Dimensional numbers during the experimental tests

15 mm glass Raschig rings	Min	Max
Reynolds number (Re_v)	46	189
Schmidt number (Sc_v)	0.58	0.59
Sherwood number (Sh_v)	1.3	5.8
$\frac{1}{2}''$ ceramic Berl saddles	Min	Max
Reynolds number (Re_v)	36	124
Schmidt number (Sc_v)	0.58	0.59
Sherwood number (Sh_v)	0.8	2.8
$\frac{1}{2}''$ ceramic Novalox saddles	Min	Max
Reynolds number (Re_v)	19	118
Schmidt number (Sc_v)	0.58	0.59
Sherwood number (Sh_v)	0.3	2.2

Though the Onda et al. correlation was the one that better predicted the experimental data, it was found that a better fit could be obtained by simply modifying the constant C to an adequate value. Fig. 6 compares the experimental results with the modified Onda correlation for the three packings analyzed. The constant C was calculated by a linear regression analysis of the data and the values 5.44, 5.91 and 7.06 were obtained for the Raschig rings, Berl saddles and Novalox saddles, respectively. The corrected correlation fits the data with an average deviation of 5, 6 and 7% for the Raschig rings, Berl saddles and Novalox saddles, respectively. Moreover 95% of the points fall within ±12% for the Raschig rings and Berl saddles and within ±15% for the $\frac{1}{2}''$ ceramic Novalox saddles.

The proposed corrected correlations for the packings analyzed could be used to design packed columns in AARS.

5. Conclusions

In this paper an experimental investigation of mass transfer performance of 15 mm glass Raschig rings, $\frac{1}{2}''$ ceramic Berl saddles and $\frac{1}{2}''$ Novalox saddles random packings for ammonia rectification in ammonia–water absorption refrigeration systems has been presented. An experimental facility was designed and built to study the ammonia–water purification process in packed columns. The facility operates at the normal operating conditions found in the high pressure stage of a small power ammonia–water absorption refrigeration system. The packed column test-rig has been tested as a rectifying section at total reflux and different operating conditions.

Experimental results for the volumetric mass transfer coefficient in the vapour phase for the packings analyzed are reported. The results are compared with different mass transfer correlations proposed in the literature. It has been found that the differences are considerable with most of these correlations, but the Onda et al. correlation predicts reasonable well the experimental results. However, a better fit of the experimental data can be obtained by changing the value of the constant of the mass transfer correlation of Onda et al. from 5.23 to 5.44, 5.91 and 7.06 for the 15 mm glass Raschig rings, $\frac{1}{2}''$ ceramic Berl saddles and $\frac{1}{2}''$ ceramic Novalox saddles, respectively. The average

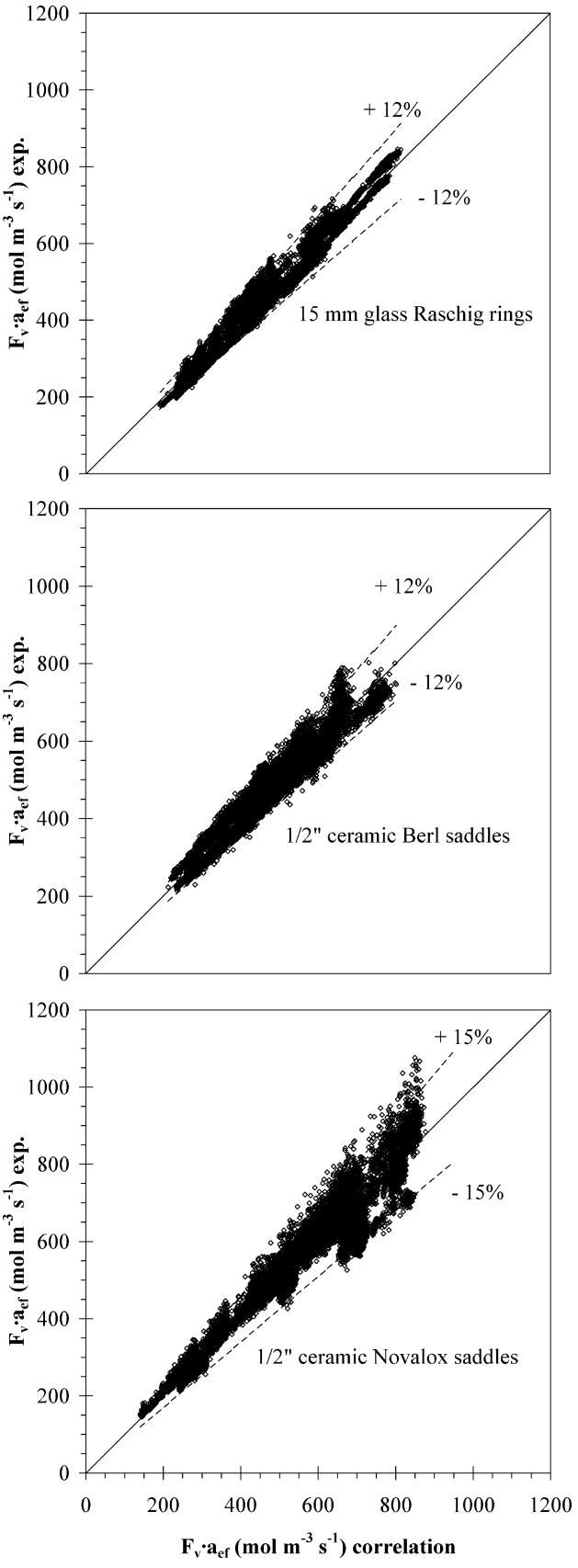

Fig. 6. Comparison between the experimental volumetric mass transfer coefficients ($F_v \cdot a_{ef}$) and those obtained with the corrected correlation of Onda et al. for 15 mm glass Raschig rings, $\frac{1}{2}''$ ceramic Berl saddles and $\frac{1}{2}''$ ceramic Novalox saddles.

deviation of the corrected correlation and the experimental values is of 5% for 15 mm glass Raschig rings, 12% for $\frac{1}{2}''$ ceramic Berl saddles and 27% for $\frac{1}{2}''$ ceramic Novalox saddles. Moreover 95% of the points fall within ±12% for the Raschig rings and Berl saddles and within ±15% for the $\frac{1}{2}''$ ceramic Novalox saddles.

Acknowledgements

The authors would like to acknowledge the financial support from the "Ministerio de Ciencia y Tecnología" (Project DPI2002-04536-C02-02).

References

[1] K. Stephan, History of absorption heat pumps and working pair developments in Europe, Int. J. Refrig. 6 (1983) 160–166.
[2] M.J. Molina, F.S. Rowland, Stratospheric sink for chlorofluoromethanes: chlorine atom-catalysed destruction of ozone, Nature 249 (1974) 810–812.
[3] J.T. McMullan, Refrigeration and the environment-issues and strategies for the future, Int. J. Refrig. 25 (2002) 89–99.
[4] F. Ziegler, State of the art in sorption heat pumping and cooling technologies, Int. J. Refrig. 25 (2002) 450–459.
[5] P. Colonna, S. Gabrielli, Industrial trigeneration using ammonia–water absorption refrigeration systems (AAR), Appl. Thermal Engrg. 23 (2003) 381–396.
[6] J. Bassols, B. Kuckelkon, J. Langreck, R. Schneider, H. Veelken, Trigeneration in the food industry, Appl. Thermal Engrg. 22 (2002) 595–602.
[7] A. Apte, Ammonia absorption refrigeration plants for the new millennium, Transparent Energy Systems Private Limited (TESPL), www.tespl.com, 2006.
[8] I. Horuz, T.M.S. Callander, Experimental investigation of a vapour absorption refrigeration system, Int. J. Refrig. 27 (2004) 10–16.
[9] J. Fernández-Seara, A. Vales, M. Vázquez, Heat recovery system to power an onboard NH_3–H_2O absorption refrigeration plant in trawler chiller fishing vessels, Appl. Thermal Engrg. 18 (1998) 1189–1205.
[10] J. Fernández-Seara, J. Sieres, M. Vázquez, Absorption refrigeration prototype for onboard cooling production in fishing vessels, in: R. Wang, Z. Lu, W. Wang, X. Huang (Eds.), Proceedings of the International Sorption Heat Pump Conference, ISHPC2002, Science Press, Shanghai, China, 2002, pp. 130–135.
[11] J. Fernández-Seara, J. Sieres, M. Vázquez, Compression–absorption cascade refrigeration system, Appl. Thermal Engrg. 26 (2005) 502–512.
[12] M.J.P. Bogart, Pitfalls in ammonia absorption refrigeration, Int. J. Refrig. 5 (1982) 203–208.
[13] J. Fernández-Seara, J. Sieres, The importance of the ammonia purification process in ammonia–water absorption systems, Energy Conv. Manag. 47 (2006) 1975–1987.
[14] M.J.P. Bogart, Ammonia Absorption Refrigeration in Industrial Processes, Gulf Publishing Company, Houston, 1981.
[15] A. Mersmann, A. Deixler, Packed columns, German Chem. Engrg. 9 (1986) 265–276.
[16] J. Fernández-Seara, J. Sieres, M. Vázquez, Distillation column configurations in ammonia–water absorption refrigeration systems, Int. J. Refrig. 26 (2003) 28–34.
[17] J. Fernández-Seara, J. Sieres, M. Vázquez, Simultaneous heat and mass transfer of a packed distillation column for ammonia–water absorption refrigeration systems, Int. J. Thermal Sci. 41 (2002) 927–935.
[18] J. Sieres, J. Fernández-Seara, Evaluation of the column components size on the vapour enrichment and system performance in small power NH_3–H_2O absorption refrigeration machines, Int. J. Refrig. 29 (2006) 579–588.
[19] G.Q. Wang, X.G. Yuan, K.T. Yu, Review of mass-transfer correlations for packed columns, Indust. Engrg. Chem. Res. 44 (2005) 8715–8729.
[20] K. Onda, H. Takeuchi, Y. Okumoto, Mass transfer coefficients between gas and liquid phases in packed columns, J. Chem. Engrg. Jpn. 1 (1968) 56–62.
[21] J.L. Bravo, J.R. Fair, Generalized correlation for mass transfer in packed distillation columns, Industrial Engrg. Chem. Process Design Development 21 (1982) 162–170.
[22] W.L. Bolles, J.R. Fair, Performance and design of packed distillation columns, Inst. Chem. Engrg. Symp. Ser. 56 (1979) 35.
[23] R. Billet, M. Schultes, Prediction of mass transfer columns with dumped and arranged packings: updated summary of the calculation method of Billet and Schultes, Chem. Engrg. Res. Design 77 (1999) 498–504.
[24] S. Piché, B.P.A. Grandjean, F. Larachi, Reconciliation procedure for gas–liquid interfacial area and mass-transfer coefficient in randomly packed towers, Indust. Engrg. Chem. Res. 41 (2002) 4911–4920.
[25] J. Sieres, J. Fernández-Seara, F.J. Uhía, M. Vázquez, Preliminary experimental results of ammonia–water rectification in packed columns at total reflux, in: J.P. Meyer, A.G. Malan (Eds.), Proceedings of the 4th International Conference on Heat Transfer, Fluid Mechanics and Thermodynamics, HEFAT 2005, Cairo, Egypt, 2005. Paper number: SJ5.
[26] J. Sieres Atienza, Estudio teórico y experimental de los procesos de transmisión de calor y transferencia de masa en columnas de destilación empacadas para sistemas de refrigeración por absorción con amoníaco–agua, Ph.D. thesis, University of Vigo, Spain, 2005.
[27] B. Ziegler, Ch. Trepp, Equation of state of ammonia–water mixtures, Int. J. Refrig. 7 (1984) 101–106.
[28] R.B. Bird, W.E. Stewart, E.N. Lightfoot, Transport Phenomena, second ed., John Wiley & Sons, New York, 2002.
[29] R. Taylor, R. Krishna, Multicomponent Mass Transfer, John Wiley & Sons, New York, 1993.
[30] J.H. Wiegand, The simplified calculations on diffusional processes, Trans. AIChE 36 (1940) 679–681.
[31] ISO, Guide to the expression of uncertainty in measurement, International Organization for Standardization (ISO), 1995.